Macromolecules

ARTICLE

pubs.acs.org/Macromolecules

Simultaneous Photoinduced Silver Nanoparticles Formation and Cationic Polymerization of Divinyl Ethers

Wayne D. Cook,*[,†] Quoc Dat Nghiem,[†] Qizhi Chen,[†] Fei Chen,[†] and Marco Sangermano[‡]

[†]Department of Materials Engineering, Monash University, Clayton, Victoria, 3800, Australia

[‡]Department of Materials Science and Chemical Engineering, Politecnico di Torino, Torino, Italy

ABSTRACT: The cationic photopolymerization of triethylene glycol divinyl ether and concomitant formation of silver particles by the use of radical photoinitiators (BAPO and BEE) and an organosoluble silver salt ($AgSbF_6$) are reported for the first time. The rate of photopolymerization is increased with higher concentrations of BEE, but the effect of $AgSbF_6$ concentration is more complex. A localized surface plasmon resonance due to the formation of silver particles was observed very shortly after the commencement of irradiation, and the maximum absorption was found to increase with irradiation time as the particle concentration and size grew. The simultaneous formation of the polymer also stabilizes the particles and prevents their agglomeration. After a certain irradiation period, the maximum absorption reaches a plateau, prior to depletion of either silver ion or photoinitiator, suggesting that the formation of the polymer matrix may restrict silver particle growth. TEM studies reveal the presence of ~10 nm diameter, crystalline silver nanoparticles, and SAXS also confirms the presence of these nanoparticles.

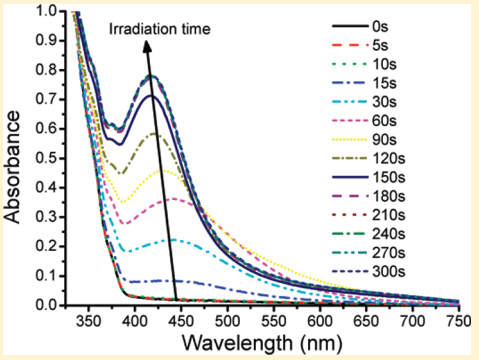

INTRODUCTION

For the past two decades, there has been considerable interest in metallic nanoparticles in applications for quantum dots and homogeneous superconductors, for magneto-optics, and opto-electronics, and for chemical and biosensors and other devices.[1−4] One of the interesting optical phenomena of metallic nanoparticles is that of localized surface plasmon resonance which is observed as strong absorptions in the UV−vis−NIR spectrum due to the collective oscillation of the conduction electrons in the electromagnetic field.[5,6] Since the electromagnetic field can only penetrate a certain depth (~50 nm for Ag[7]), the surface electrons are the most important except for small particles. The effect of the silver particle size, shape, and containing medium on the localized surface plasmon resonance is rather complex. Summarizing the literature up to the mid-1980s, Bohren and Huffman[5] report that the plasmon resonance is red-shifted (shifted to longer wavelengths) as the particle size increases, and this has been further documented by Kreibig and Genzel.[8] Thus, in a recent study of the aqueous formation of silver from silver nitrate (the silver cation acting as the oxidizer) and trisodium citrate (acting as a reducer) in acid, the observed decrease in the wavelength maximum (a blue shift) as the concentration of citrate increased was interpreted by Smitha et al.[9] as a decrease in the particle size. However, Manikandan et al.[10] reported a blue shift as the diameter of silver nanoparticles in a ceramic increased. Regarding shape, as the particles become more spherical, the absorption maximum wavelength is predicted to decrease (i.e., the absorption is blue-shifted)[11] and to lower the absorption than less spherical particles such as cubes or rods, for example. The refractive index of the particle coating or of the embedding medium also has an influence on the plasmon resonance and causes a red-shift as the index increases.[5,6,12]

One of the most useful ways of utilizing the properties of metallic nanoparticles is in the form of polymer composites, and those containing silver or gold particles offer unusual spectroscopic properties, high conductivity, and antibacterial activity. Although nanocomposites were initially prepared from separately formed nanoparticles and a polymer,[13−16] *in situ* formation of both the polymer and metallic particle provides a greater range of potential polymeric materials and a greater control of the particle size and distribution. Carotenu et al.[17] synthesized silver nanocomposites in poly(vinylpyrrolidone) using ethylene glycol as the solvent and reducer and suggested that they could be used for advanced optical applications. De Santa Maria et al.[18] manufactured silver nanoparticles in aqueous dispersions of styrene−divinyl particles for bactericidal applications by reduction of the silver salt with hydroxylamine. In order to create a composite that protects against biological warfare agents, Wu et al.[19] prepared aqueous dispersions of inorganic−organic hybrids incorporating silver nanoparticles by hydrazine reduction of $AgNO_3$.

Recently studies of solvent-free metal−polymer nanocomposites formed *in situ* have employed thermally activated initiators to form the radical which can acts as the reducing agent. For example, several authors[20,21] have used azobis(isobutyronitrile) as the thermal initiator to form a poly(urethane acrylate-*co*-styrene) network and silver particles. Brito-Silva et al.[22] studied

Received: March 14, 2011
Revised: May 2, 2011
Published: May 06, 2011

the formation of silver nanoparticles from silver nitrate in unsaturated polyester resins that were thermally cured with methylethyl ketone peroxide. Interestingly, these systems did not form silver particles when the thermal cured at 40 °C in the dark initiator, but they did form nanoparticles when postcured to 80 °C or after UV irradiation. In the former case, a single plasmon resonance peak near 410 nm was found which did not shift in position with postcuring time or silver salt concentration, but two peaks at 410 and 470 nm were observed in the photoirradiated systems which was attributed to particle aggregation. The absorbances at the peak maximum increased with heating or irradiation time and with the concentration of the silver salt. In addition, a small blue shift in the absorption peak was reported during the postcuring or irradiation, but no explanation was provided.

Sangermano, Yagci, and Rizza[23−26] have developed a unique technique for forming silver and gold nanoparticles *in situ* during photopolymerization of acrylates and epoxies by reduction of the metal salt by a carbon radical arising from a benzoin-based photoinitiator. Many free radical photoinitiators are capable of reducing silver salts. For example, benzoin methyl ether (used in the present work) is a commonly used photoinitiator and is photolyzed into a benzoyl radical and a methoxyphenylmethyl radical. Wayner et al.[27] reported the oxidation potential of the methoxyphenylmethyl radical to be −0.09 V (relative to the standard hydrogen electrode). Since the oxidation potential (i.e., relative to the standard hydrogen electrode) for the aqueous silver ion is +0.8 V,[28] the free energy energy change for the oxidation of Ag^+ by the methoxyphenylmethyl radical is −87 kJ/mol and is therefore very favorable. In a study of the photo-induced formation of silver particles in a cationically cured aliphatic epoxy matrix, Yagci et al.[25] found that the silver particles in the epoxy nanocomposites had a size distribution ranging between 20 and 40 nm and that an increase in the silver salt concentration did not significantly affect the size of the nanoparticles but increased the density of nanoparticles. In another paper on gold particle formation from a gold salt in a similar epoxy matrix, Yagci et al.[26] reported that when the gold ion concentration was low, almost all of the particles were 1−2 μm size and only a few nanoparticles were between 30 and 60 nm, but at a higher concentration, the particles size ranged from 50 to 60 nm.

Balan et al.[29] have prepared silver nanoparticles *in situ* during the photopolymerization of poly(ethylene glycol) dimethacrylate using a diaminofluorene derivative as the photoreducer. The one-to-one reaction between the excited photoinitiator and the silver ion was demonstrated in acetonitrile by the presence of an isosbestic point between the silver plasmon resonance peak and the diaminofluorene peak. In a related study[30] eosin-Y (a xanthene species) was used as the photoreducer for the silver salt. Lee and Tsao[31] have prepared silver−acrylic acid/poly(ethylene glycol)/methyl ether acrylate hydrogel composites by photoinitation of the polymerization and *in situ* formation of the silver. It is interesting to note that these workers suggested that the reduction of the silver ions was due to the photoredox reaction of a complex of pyrrolidone and the silver salt rather than by the radicals formed from the diethoxyacetophenone initiator used.

To the authors' knowledge, there have been no reports on the simultaneous photoinduced silver deposition and cationic polymerization of divinyl ethers. Such a study, for example with triethylene glycol divinyl ether (TEGDVE, as shown in Scheme 1) and the non-nucleophilic SbF_6^- anion of Ag^+, is of particular interest because the etheric groups in the monomer aid the solubility of the silver salt and because TEGDVE is very rapidly and efficiently polymerized by carbocations[32] such as those that should be produced by the oxidation of a photoinitiator radical.

Scheme 1. Materials Used

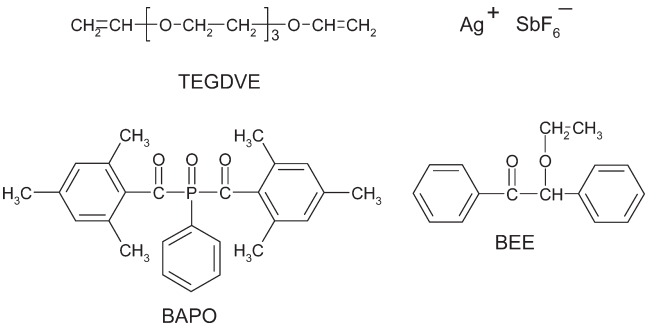

EXPERIMENTAL SECTION

Materials. The cationic polymerization of triethylene glycol divinyl ether (TEGDVE, Aldrich) was performed via the photoredox system of either 1 wt % bis(2,4,6-trimethylbenzoyl)phenylphosphine oxide (BAPO, supplied as Irgacure 819 by Ciba) and 3 wt % silver hexafluoroantimonate ($AgSbF_6$, Aldrich) or with 0.5 or 1 wt % benzoin ethyl ether (BEE, Aldrich) and 1.5 or 3 wt % $AgSbF_6$, and their structures are shown in Scheme 1. Diphenyliodonium hexafluorophosphate (Ph_2IPF_6, Aldrich) and camphorquinone (CQ, Aldrich) were used as a nonmetallic cationic photoinitiating system.[32] All these materials were used as received.

Photo-DSC. Isothermal photopolymerization studies were performed in a Perkin-Elmer DSC-7, calibrated for temperature and enthalpy using high purity zinc and indium standards. The instrument was modified[33] to allow the irradiation of both the sample and reference DSC pans, minimizing the thermal imbalance created by the radiation source. A poly(methyl methacrylate) (PMMA) block, with holes located directly above the DSC pan holders, was used in place of the standard DSC cover. The systems were photopolymerized using attenuated radiation from a tungsten−mercury−halide Polilight PL400 (Rofin, Australia) radiation source and fiber optic, which has selectable wavelength regions defined by cut-off and cut-on filters. The wavelength regions were either 350−360 nm radiation for BEE with an intensity of ∼2 mW/cm^2 or 390−440 nm (maximum at 415 nm) for BAPO at an intensity of ∼0.5 mW/cm^2, as measured with an Ocean Optics USB2000 fiber-optic spectroradiometer at the base of the DSC pan. The radiation was directed into a bifurcated quartz fiber optic light guide, the legs of which were fitted into the holes in the PMMA block. Fine aluminum rings were placed on the ledge in each sample pan holder, and two 0.05 mm thick poly(ethylene terephthalate) (PET) covers (6 mm diameter) with two vent holes were used to cover the DSC pan holders to prevent an unstable baseline and to minimize sample evaporation during the experiment. Any remaining thermal imbalance in the heat from the lamp onto the two pans was further corrected by repeating the illumination of the cured sample and reference in a second isothermal DSC run and subtracting the data from the first run—subsequent polymerization was not observed during the repeated illumination. All samples were photocured at 50 °C under a N_2 atmosphere at a flow rate of 20 mL min^{-1}. To obtain stability of the radiation intensity, the light source was activated 60 s before commencement of irradiation by use of a shutter in front of the light guide. Sample masses of ∼3 mg were used. BEE and BAPO have maximum absorptions at 328 and 367 nm in ethanol, respectively, and at the wavelength of the Polilight

dx.doi.org/10.1021/ma200575n |*Macromolecules* 2011, 44, 4065–4071

(either 350−360 or 415 nm for BEE or BAPO, respectively), the absorptions are reduced by about 50%; so for the ∼0.4 mm thick specimens used in the photo-DSC experiments the attenuation with depth into the samples can be ignored.

The measured heat flow is proportional to the conversion rate, so that the rate of conversion ($d\alpha/dt$) can be defined as follows:

$$\frac{d\alpha}{dt} = \frac{1}{\Delta H_{tot}}\left(\frac{dH}{dt}\right)_T \quad (1)$$

where $(dH/dt)_T$ is the measured heat flow at a constant temperature T and ΔH_{tot} is the total exothermic heat of reaction. On the basis of the heat of cationic polymerization for butyl vinyl ether[34,35] of 60 kJ/mol, the theoretical heat for complete of polymerization of TEGDVE was calculated as 593 J/g using its theoretical molecular weight.

UV−vis Spectrometry. A Cary 3000-Bio spectrometer (Varian, Australia) was used to measure the UV−vis spectra of the reagents using a 10 mm path length cell using a scan rate of 600 nm/min. The monomer TEGDVE showed significant absorption below 330 nm, which appears to be due to the presence of stabilizers in the monomer. The spectra of 0.1 wt % $AgSbF_6$ in ethanol showed virtually no absorption down to 300 nm with substantial absorption only below 270 nm. The photoinitiator BAPO had absorption maxima at 367 nm, a shoulder at 396 nm, and a tail ending around 440 nm, whereas BEE showed an absorption maximum at 328 nm, a strong absorption at 365 nm, and a tail ending near 385 nm.

The spectrophotometer was also used to observe the changes in the spectroscopic extinction (i.e., absorption and scattering[7]) of fully formulated resin systems during irradiation at room temperature with the attenuated radiation from the Polilight PL400 using wavelengths of 350−360 nm for BEE amd 390−440 nm for BAPO at an intensity of ∼0.1 mW/cm^2 at the surface of the resin. The resin was contained in thin cells (either 0.08 mm for resins formulated with BAPO or ∼0.5 mm thick for BEE) constructed from two quartz microscope slides separated by a PTFE gasket. An identical cell containing ethanol was used as the reference. The specimen was periodically irradiated, and then the spectrum was immediately measured. Although extended time periods (tens of minutes) between each irradiation were found to have a small effect on the growth rate of the plasmon absorbance, the effect of the 1 min interval required to perform the UV−vis measurement was found to be negligible.

The importance of scattering to the overall extinction was evaluated by shifting the sample plus cell 10 cm closer to the detector—since no significant decrease in extinction was observed, the spectroscopic changes can be attributed solely to the absorption phenomenon, and so the Beer−Lambert law applies.[12,36−40]

TEM Results. TEGDVE/$AgSbF_6$/BEE samples were photocured at room temperature by irradiation for 1 min each side using the unattenuated 350−360 nm band of the Polilight 400. The resulting polymer was embedded in a mounting epoxy resin and sectioned using a Reichert Ultracut-S cryo-ultromicrotome to produce ∼70 nm thickness. The sections were studied by transmission microscopy using a Philips CM20 transmission electron microscope, and selected regions of the sample containing 10 wt % $AgSbF_6$ were used to perform electron diffraction studies, using a camera length of 1.4 m and an accelerating voltage of 200 kV.

XRD. WAXS/SAXS studies were undertaken at Anton Paar, Austria, using the SAXSess mc^2 SAXS platform in transmission mode. The X-ray generator was a ID3003 (Cu Kα, λ = 0.1542 nm) using a power of 40 kV at 50 mA, a 0.3 mm × 20 mm line beam collimation, an image plate detector, 5 min exposure time, and a TCS 120 standard sample holder for solids. The TEGDVE resin was formulated with 1 wt % BEE and either 3, 5, or 10 wt % $AgSbF_6$, and the 0.5 mm thick samples were photopolymerized using the 350−360 nm Polilight radiation for 1 min on each side. For a reference without silver particles, TEGDVE was photopolymerized with 0.2 wt % Ph_2IPF_6 and 1 wt % CQ at room temperature using 470 nm radiation (which corresponds to the absorption maximum of CQ) for 2 min on each side.

Scheme 2. Photolysis of BEE and BAPO and the Mechanism of Photoinduced Reduction of Ag^+ and Cationic Polymerization of TEGDVE Monomer

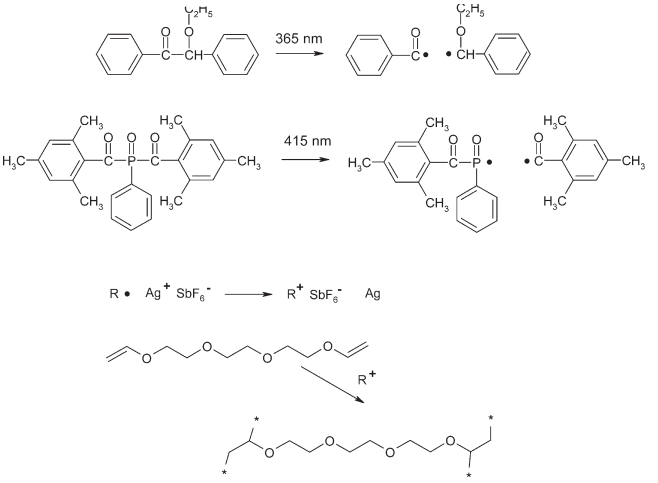

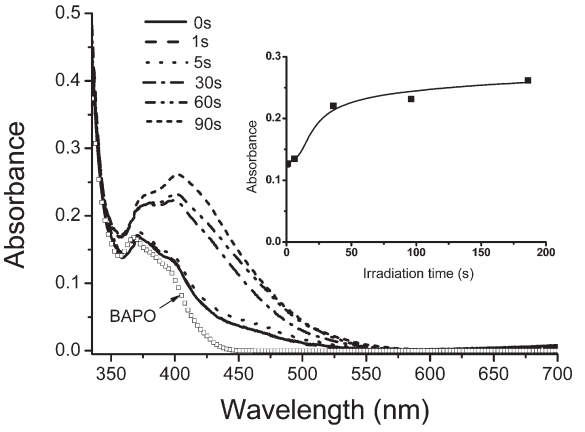

Figure 1. UV−vis spectrum during irradiation of a ∼0.08 mm thick sample of TEGDVE/1 wt % BAPO/3 wt % $AgSbF_6$ using 415 nm radiation. A plot of the absorbance spectrum of BAPO is included and is scaled to the absorbance of the formulated resin at a wavelength of ∼370 nm. The inset shows the increase in the plasmon absorption at 402 nm with irradiation time.

RESULTS AND DISCUSSION

The photolysis process for BAPO[41] and for BEE[42] and the mechanism for photocationic polymerization of TEGDVE and simultaneous reduction of the silver ions using are shown in Scheme 2. It should be noted that free radical polymerization of vinyl ethers is slow even at elevated temperatures,[43] and so the polymerization process is entirely by cationic polymerization.

Figure 1 shows the changes in the UV−vis spectra during 415 nm irradiation of the TEGDVE/1 wt % BAPO/3 wt % $AgSbF_6$ system. After 5 s of irradiation, a new absorbance appears near 400 nm which overlaps with the spectrum of BAPO which is similar to that observed by Jradi et al.[44] in their study of the

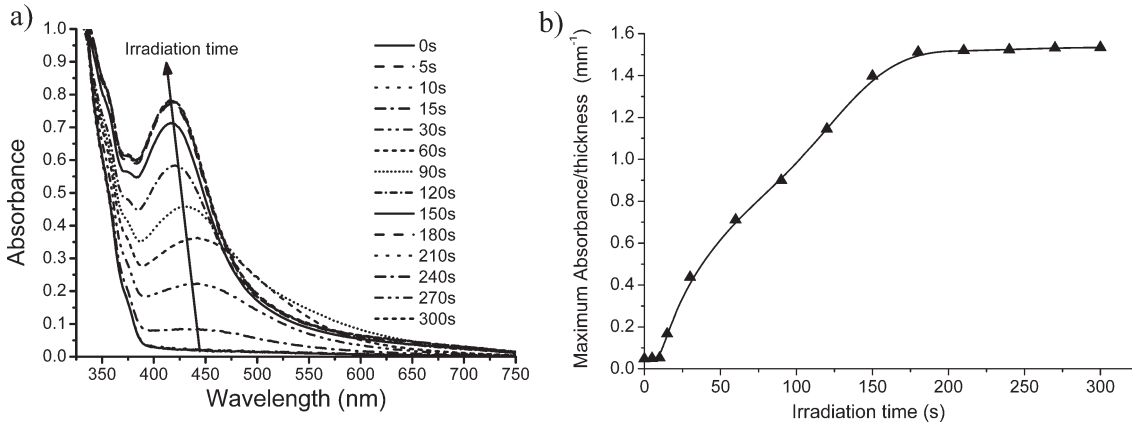

Figure 2. (a) UV−vis spectra of a 0.51 mm thick specimen of TEGDVE/3 wt % $AgSbF_6$/1 wt % BEE during irradiation of BEE at 360 nm. (b) Absorbance peak height per unit thickness versus irradiation time.

photoreduction by BAPO of silver nitrate in isopropanol containing poly(vinylpyrrolidone) as stabilizer to prevent particle aggregation. The peak near 400 nm can be identified as being due to the silver plasmon resonance which is commonly observed for silver nanoparticles.[5] Only one new peak is obvious in the spectrum, and this suggests that the particles are not very elongated because distinctive splitting of the peak has been observed[3,5] with particles having aspect ratios as low as 2.5. In relation to this, Jradi et al.[44] found that the photoreduction by BAPO of silver nitrate in the absence of poly(vinylpyrrolidone) caused a very large red shift (∼400 nm) due to particle agglomeration, and so it appears that in our system the polymer matrix that forms during the photoirradiation also acts as a particle stabilizer. Figure 1 shows there is a short induction period before any changes occur in the spectrum. This induction could be due to radical scavenging by residual inhibitors in the resin which temporarily prevent silver ion reduction. Alternatively, this induction may correspond to the inhibition of the triplet state of the BAPO by residual oxygen, by analogy with the work by Balan et al.[29] on a diaminofluorene derivative.

The inset in Figure 1 indicates that after the induction period the plasmon absorption rises rapidly and then approaches a plateau after ∼50 s irradiation. Provided that the extinction is caused by the absorption of small nanoparticles and not particles larger than 50 nm,[7] the absorption can be used as a measure of the concentration of silver atoms formed in the nanoparticles.[12,36−40] Thus, it appears that after ∼50 s irradiation there is no more growth of the nanoparticles. This is not caused by attenuation of the radiation by the increased absorption caused by the plasmon resonance because Figure 1 reveals that the percent transmittance of the 415 nm radiation (the irradiating wavelength) by the 0.08 mm thick film has only decreased from ∼83% before commencement of irradiation to ∼56% after irradiation. Also, this effect is not caused by depletion of BAPO photoinitiator because the absorption due to BAPO is still obvious in the spectrum after cessation of irradiation. In addition, depletion of silver ions by the radicals is unlikely to be responsible because in this system the molar ratio of silver ions to BAPO molecules is 3.7:1 and the diacylphosphine oxide BAPO molecule generates in theory one phenyl ketone radical and a phosphonyl radical per photon,[41] and so there appears to be an excess of radicals available. Although the quantum efficiency of BAPO does not appear to be known, for the related but monoacylphosphine oxide, 2,4,6-trimethylbenzoyldiphenylphosphine oxide, Decker[45] quotes a quantum yield of 0.8 radicals per photon so that the ratio of silver ions to reducing radical should be even greater that that calculated above. Another potential explanation is that the absorbance plateau occurs when the silver particles grow to such a size that most of the atoms do not undergo plasmon resonance[7,11] but are only involved in scattering the radiation; however, experiments performed by locating the sample closer or further from the detector did not significantly alter the spectrum and so failed to give any evidence of radiation scattering. A more likely reason for the absorbance plateau is that the change in mobility of the ions, atoms, and radicals due to the formation of the matrix prevents their ready diffusion—in fact, we have shown that the polymer of TEGDVE is in the glass transition region[43] with a modulus of ∼10^8 Pa at room temperature (the condition of the spectroscopy experiment), and so ion/radical diffusion may be slow.

The radical-generating system, BAPO, is not ideal for observing the plasmon resonance phenomenon due to the overlap of the BAPO and silver spectra, and so experiments were performed with BEE as the initiator because BEE does not absorb appreciably above 385 nm. Figure 2 shows that immediately after commencement of the UV irradiation the BEE peak near 350 nm starts to decrease. At the same time, the plasmon resonance absorption peak near 425 nm, due to the formation of the silver particles, increases up to a plateau value during the irradiation period, as was observed with the system containing BAPO. Similarly to the case of BAPO, this plateau is unlikely to be due to depletion of silver ions because the molar ratio of Ag^+ to BEE is 2.1:1, and assuming that both radicals derived from BEE are effective and that the quantum yield of radicals per photon is only 0.68,[42] there should be an excess of silver ions.

Figure 2 also reveals that the wavelength of the plasmon resonance absorption peak is blue-shifted as the peak grows. This is unexpected because plasmon resonance is usually slightly red-shifted as the particle size increases.[5,6,12] In addition, during polymerization of vinyl monomers, the refractive index of the medium increases[46−48] and an increase in the refractive index of the medium suspending the silver particles also normally causes a red-shift.[5,6] However, if the particles become more spherical, then a blue shift is expected.[11] In addition, the breadth of the absorption appears to narrow, and this is particularly noticeable after 30 s of irradiation. Similar behavior has been reported by Kreibig and Genzel,[8] but the reason for this does not appear to be clear.

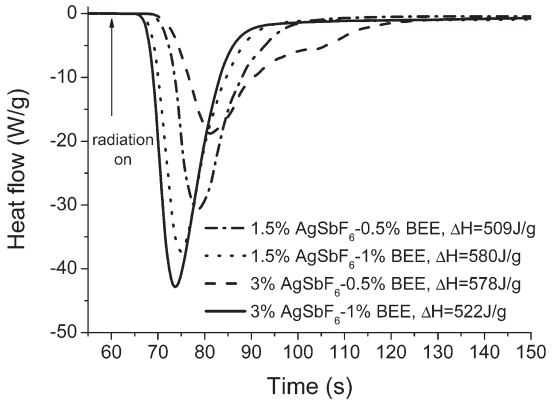

Figure 3. Photo-DSC of TEGDVE with varying amounts of $AgSbF_6$ and BEE at 50 °C and using the Polilight band 350−360 nm.

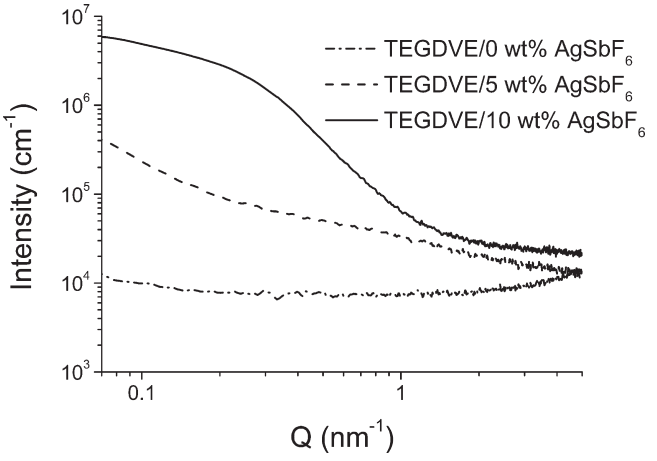

Figure 4. Small-angle X-ray diffraction pattern of photocured samples formed from TEGDVE/$AgSbF_6$/1 wt % BEE using 0, 5, and 10 wt % $AgSbF_6$. The data for the latter two have been background corrected by subtracting the pattern for the cured TEGDVE sample.

The photocuring behavior of TEGDVE/$AgSbF_6$/BEE with 360 nm radiation is shown in Figure 3, and it is seen that the polymerization is complete in less than 2 min. It is of interest that the maximum curing rate (38 W/g) and the time (∼25 s) required for "full" cure for TEGDVE/1.5 wt % $AgSbF_6$/1 wt % BEE was similar to that previously measured for the camphorquinone-iodonium photoinitiating system TEGDVE/1 wt % Ph_2IPF_6/1 wt % CQ (47 W/g and ∼40 s) studied previously.[32] Although, it is difficult to make a quantitative comparison of photocuring data where different photoinitiating systems are used, an estimate of the power absorbed per unit volume by the initiating systems can be made from the concentration of photoinitiator (1 wt % BEE, 1 wt % CQ), the absorbance per unit thickness of sample at the relevant wavelength (∼1.2 per mm path length at 350 nm for BEE and ∼0.1 per mm path length for CQ[32]), and the irradiance at the sample surface (2 mW/cm^2 for irradiation of BEE at 350−360 nm and 80 mW/cm^2 for irradiation of CQ at 400−500 nm[32]), since the concentration of photo-oxidizer (1.5 wt %$AgSbF_6$ and 1 wt % Ph_2IPF_6) is similar in each system. The power absorbed per unit volume is calculated to be 2.6 and 8 W/cm^3 for the $AgSbF_6$/1 wt % BEE and Ph_2IPF_6/1 wt % CQ systems, respectively, and the similarity of these values suggests

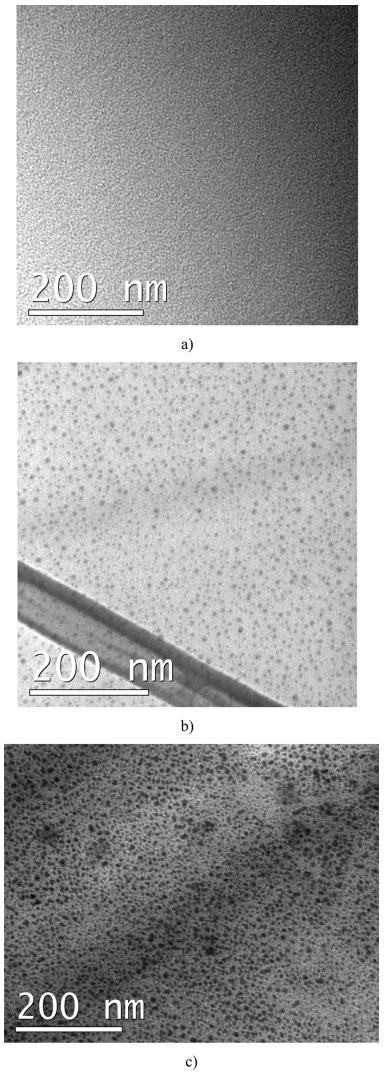

Figure 5. TEM image of silver nanoparticles deposited in a cross-linked TEGDVE matrix formed from TEGDVE/$AgSbF_6$/1 wt % BEE using (a) 3, (b) 5, and (c) 10 wt % $AgSbF_6$. The diagonal bar in image (b) is an artifact.

that the current photoredox system has similar efficiency to the Ph_2IPF_6/CQ system.

Figure 3 also shows that with $AgSbF_6$ as the oxidant photopolymerization does not occur until ∼5 s after commencement of irradiation, and this may be due to trace basic impurities such as amines that may consume the carbocations which are formed by oxidation of the radicals by the silver ions. Alternatively, this induction behavior may be caused by radical scavenging by impurities in the components. The rate of reaction in the early stages of the reaction and the maximum rate of reaction increase in the same order:

3 wt % $AgSbF_6$/1 wt % BEE > 1.5 wt % $AgSbF_6$/1 wt % BEE

> 1.5 wt % $AgSbF_6$/0.5 wt % BEE

> 3 wt % $AgSbF_6$/0.5 wt % BEE

The higher rate of polymerization for the systems with 1 wt % BEE is understandable because the rate of production of radicals is dependent on the concentration of BEE in the matrix.

dx.doi.org/10.1021/ma200575n |*Macromolecules* 2011, 44, 4065–4071

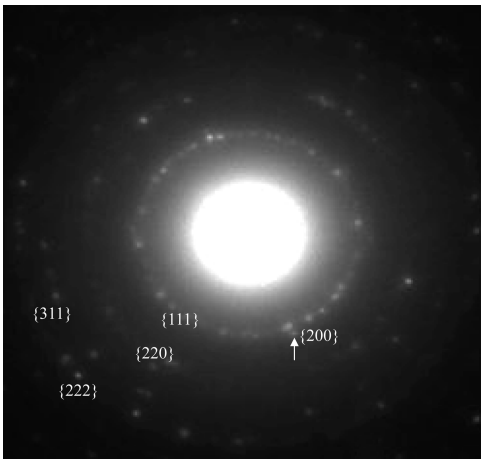

Figure 6. TEM selected area diffraction pattern of a photocured sample of TEGDVE/10 wt % $AgSbF_6$/1 wt % BEE. The {*hkl*} planes are identified in the image.

However, the reason for differing effects of the silver ion concentration on the cure rate for the systems with 1 and 0.5 wt % BEE is less clear but may be associated with the kinetics of the consumption of the BEE radicals by the silver ions. The heat of polymerization (see Figure 3) is approximately 550 ± 40 J/mol, which is close to the theoretical expected heat of polymerization of 593 J/g.[34,35] This might be expected because TEGDVE polymerizes to forms a leathery polymer which at 50 °C is in the rubbery state,[43] and so molecular motion and polymerization are possible up to high degrees of cure without vitrification effects.

Since the plasmon resonance behavior suggests the presence of silver nanoparticles in the polymer matrix, it was of interest to establish if further information could be obtained by X-ray diffraction. Figure 4 shows the small-angle X-ray diffraction data for cured specimens with 0, 5, and 10 wt % $AgSbF_6$. The sample containing no silver shows minimal scattering as expected, but the samples with silver show significant scattering at Q values of less than 1 nm^{-1}, indicating particles with diameters of more than 1 nm.

Figure 5 shows TEM images of ultramicrotomed samples of photocured TEGDVE with varying amounts of BEE and $AgSbF_6$. The sample prepared with 3 wt % of $AgSbF_6$ does not show any clear evidence of silver particles, but as the amount of the silver salt is raised, the presence of nanosized (ca. 10 nm) particles of silver, which were formed during the photoinitation process, are observed. The selected area diffraction pattern of one sample (Figure 6) clearly reveals a polycrystalline ring pattern. The diffraction indices of the planes are identified in the figure—the {200} plane is close to the {111} plane and is not well-defined. The radii, r, of the rings were measured from the image, and the values of r^2 were calculated to be in the ratio of 3, 3.8, 7.4, 10.8, and 12.8, which is reasonably close to the ideal ratios of the diffraction rings from a face-centered-cubic (FCC) structure, which is 3, 4, 8, 11, and 12.[49] According to diffraction theory,[50] the lattice constant (d_{hkl}) can be determined from the expression

$$L\lambda = rd_{hkl}$$

where L is the camera length (1.4 m) and λ is the electron wavelength at 200 kV (0.025 Å). Therefore, the lattice constant was determined to be between 4.04 and 4.18 Å, which is also in agreement with the reported value of 4.07 Å for Ag.[51]

CONCLUSIONS

Silver−polymer nanocomposites have been prepared by simultaneous photoreduction of silver ions and cationic cross-linking of a divinyl ether matrix. The cationic polymerization of the vinyl ether is caused by the alkyl cations formed as a result of the oxidation of the photoinitiator carboradicals by the silver ions. The rate of photopolymerization was very fast and increased at higher concentrations of silver salt or photoinitiator.

The maximum absorbance of the plasmon resonance caused by the formation of silver particles increased during the photoirradiation process but then attained a plateau before either the photoinitiator or the silver ions were consumed. This result appears to be caused by the formation of the cross-linked polymer matrix which prevents further nanoparticle formation or growth.

Small-angle XRD confirms the presence of nanosized particles in the cross-linked matrix and TEM, and electron diffraction reveals crystalline silver nanoparticles with dimensions of the order of 10 nm.

AUTHOR INFORMATION

Corresponding Author

*E-mail Wayne.Cook@eng.monash.edu.au; Tel +613 9905 4926; Fax +613 9905 4940.

ACKNOWLEDGMENT

The authors acknowledge the Australian Research Council Grant DP1093217 for financial funding and the Monash 2009 European Travel Grant for travel funding of Prof Sangermano to Australia. The authors also thank Heiner Santner, Anton Paar GmbH, Austria, for performing the SAXS measurements and Stuart Cragg, Anton Paar Product Manager at MEP Instruments, Australia, for arranging the XRD measurements. Dr. Cornelis Moorhoff is also thanked for his helpful advice.

REFERENCES

(1) Weisbuch, C.; Vinter, B. *Quantum Semiconductor Structures-Fundamentals and Applications*; Academic Press: New York, 1991; p 252.
(2) Kirk, W. P., Reed, M. A., Eds. *Nanostructures and Mesoscopic Systems*; Academic Press: New York, 1992; p 550.
(3) Hutter, E.; Fendler, J. H. *Adv. Mater.* **2004**, *16*, 1685–1706.
(4) Sakamoto, M.; Fujistuka, M.; Majima, T. *J. Photochem. Photobiol., C* **2009**, *10*, 33–56.
(5) Bohren, C. F.; Huffman, D. R. *Absorption and Scattering of Light by Small Particles*; John Wiley and Sons: New York, 1983.
(6) Cortie, M.; Rahmani, A. *Aust. Phys.* **2009**, *46*, 42–46.
(7) Xia, Y.; Halas, N. J. *MRS Bull.* **2005**, *30*, 338–348.
(8) Kreibig, U.; Genzel, L. *Surf. Sci.* **1985**, *156*, 678–700.
(9) Smitha, S. L.; Nissamudeen, K. M.; Philip, D.; Gopchandran, K. G. *Spectrochim. Acta, Part A* **2008**, *71*, 186–190.
(10) Manikandan, D.; Mohan, S.; Magudapathy, P.; Nair, K. G. M. *Physica B* **2003**, *325*, 86–91.
(11) Gonzalez, A. L.; Noguez, C. *J. Comput. Theor. Nanosci.* **2007**, *4*, 231–238.
(12) Underwood, S.; Mulvaney, P. *Langmuir* **1994**, *10*, 3427–3430.
(13) Lee, W.-F.; Tsao, K.-T. *J. Appl. Polym. Sci.* **2006**, *100*, 3653–3661.
(14) Kuila, B. K.; Garai, A.; Nandi, A. K. *Chem. Mater.* **2007**, *19*, 5443–5452.
(15) Carotenuto, G.; Nicolais, L.; Martorana, B.; Perlo, P. Metal−polymer nanocomposite synthesis: novel ex situ and in situ approaches. In *Metal-Polymer Nanocomposites*; Nicolais, Carotenuto, G., Eds.; John Wiley & Sons: Hoboken, NJ, 2005.

(16) Donescu, D.; Nistor, C. L.; Purcar, V.; Serban, S.; Radovici, C.; Raditoiu, V.; Petcu, C.; Ghiurea, M. Silver-polymer nanohybrids prepared by microemulsion polymerization. *J. Nano Res.* **2009**, *6*, 147–156.
(17) Carotenuto, G.; Pepe, G. P.; Nicolais, L. *Eur. Phys. J. B* **2000**, *16*, 11–17.
(18) de Santa Maria, L. C.; Oliveira, R. O.; Merçon, F.; Borges, M. E. R. S. P.; Barud, H. S.; Ribeiro, S J. L.; Messaddeq, Y.; Wang, S. H. *Polimeros* **2010**, *20*, 227–230.
(19) Wu, K. H.; Chang, Y. C.; Tsai, W. Y.; Huang, M. Y.; Yang, C. C. *Polym. Degrad. Stab.* **2010**, *95*, 2328–2333.
(20) Kim, J.-Y.; Shin, D.-H.; Ihn, K.-J. *Macromol. Chem. Phys.* **2005**, *206*, 794–801.
(21) Eksik, O.; Erciyes, A. T.; Yagci, Y. *J. Macromol. Sci., Part A* **2008**, *45*, 698–704.
(22) Brito-Silva, A. M.; de Araujo, C. B.; Brayner, F. A.; Santos, S. S.; Galembeck, A.; Milet, E. R. C. *Polym. Eng. Sci.* **2010**, *50*, 2350–2355.
(23) Sangermano, M.; Yagci, Y.; Rizza, G. *Macromolecules* **2007**, *40*, 8827–8829.
(24) Yagci, Y.; Sangermano, M.; Rizza, G. *Chem. Commun.* **2008**, *24*, 2771–2773.
(25) Yagci, Y.; Sangermano, M.; Rizza, G. *Polymer* **2008**, *49*, 5195–5198.
(26) Yagci, Y.; Sangermano, M.; Rizza, G. *Macromolecules* **2008**, *41*, 7268–7270.
(27) Wayner, D. D. M.; Sim, B. A.; Dannenberg, J. J. *J. Org. Chem.* **1991**, *56*, 4853.
(28) Vanysek, P. Electrochemical Series In *Handbook of Chemistry and Physics*, 88th ed.; Chemical Rubber Co.: Boca Raton, FL, 2007.
(29) Balan, L.; Jin, M.; Malval, J.-P.; Chaumeil, H.; Defoin, A.; Vidal, L. *Macromolecules* **2008**, *41*, 9359–9365.
(30) Balan, L.; Malval, J.-P.; Schneider, R.; Le Nouen, D.; Lougnot, D.-J. *Polymer* **2010**, *51*, 1363–1369.
(31) Lee, W.-F.; Tsao, K.-T. *J. Mater. Sci.* **2010**, *45*, 89–97.
(32) Cook, W. D.; Chen, S.; Chen, F.; Kahveci, M. U.; Yagci, Y. *J. Polym. Sci., Polym. Chem.* **2009**, *47*, 5474–5487.
(33) Cook, W. D. *J. Appl. Polym. Sci.* **1991**, *42*, 2209–2222.
(34) Shostakovskii, M. F.; Bogdanov, I. F. *J. Appl. Chem. Russ.* **1942**, *15*, 249–259.
(35) Zeng, Z.; Zhang, L.; Yang, J.; Chen, Y. *J. Appl. Polym. Sci.* **2005**, *96*, 1930–1935.
(36) Swanson, N. L.; Billard, B. D. *Nanotechnology* **2003**, *14*, 353.
(37) Stepanov, A. L.; Popok, V. N.; Khaibullin, I. B.; Kreibig, U. *Nucl. Instrum. Methods Phys. Res., Sect. B* **2002**, *191*, 473–477.
(38) Rance, G. A.; Marsh, D. H.; Khlobystov, A. N. *Chem. Phys. Lett.* **2008**, *460*, 230–236.
(39) Liu, X.; Atwater, M.; Wang, J.; Huo, Q. *Colloids Surf., B* **2007**, *58*, 3–7.
(40) Al-Thabaiti, S.; Al-Nowaiser, F. M.; Obaid, A. Y.; Al-Youbi, A. O.; Khan, Z. *Colloids Surf., B* **2008**, *67*, 230–237.
(41) Jockusch, S.; Turro, N. J. *J. Am. Chem. Soc.* **1998**, *120*, 11773–11777.
(42) Lewis, F. D.; Lauterbach, R. T.; Heine, H. G.; Hartmann, W.; Rudolph, H. *J. Am. Chem. Soc.* **1975**, *97*, 1519–1525.
(43) Chen, S.; Cook, W. D.; Chen, F. *Polym. Int.* **2007**, *56*, 1423–1431.
(44) Jradi, S.; Balan, L.; Zeng, X. H.; Plain, J.; Lougnot, D. J.; Royer, P.; Bachelot, R.; Akil, S.; Soppera, O.; Vidal, L. *ACS Nano* **2010**, *4*, 4579–4586.
(45) Decker, C. *Macromol. Rapid Commun.* **2002**, *23*, 1067–1093.
(46) Dorkenoo, K.; van Wonderen, A. J.; Bulou, H.; Romeo, M.; Crégut, O.; Fort, A. *Appl. Phys. Lett.* **2003**, *83*, 2474–2476.
(47) Shostakovsky, M. F.; Gladyshevskaya, V. A. *Russ. Chem. Bull.* **1954**, *3*, 299–304.
(48) Learmonth, G. S.; Pritchard, G. *J. Appl. Polym. Sci.* **1969**, *13*, 2119–2127.
(49) Azaroff, L. V.; Buerger, M. J. *The Powder Method in X-ray Crystallography*; McGraw-Hill Book Co.: New York, 1958; p 81.
(50) Hirsch, P.; Howie, A.; Nicholson, R. B.; Pashley, D. W.; Whelan, M. J. *Electron Microscopy of Thin Crystals*; Robert E. Krieger Publishing Co.: New York, 1977; p 109.
(51) Callister, W. D. *Materials Science and Engineering: An Introduction*, 7th ed.; John Wiley & Sons: New York, 2007; p 41.